Bull. Natn. Sci. Mus., Tokyo, Ser. C, 18 (2), pp. 49–64, June 22, 1992

Chemical Compositions of Rhodonite, Bustamite and Mn-bearing Clinopyroxenes from Skarns in Japan

By

Satoshi MATSUBARA and Akira KATO

Department of Geology, National Science Museum, Tokyo

Abstract Rhodonite, bustamite and Mn-bearing clinopyroxenes from four skarn deposits in Japan were analysed using EDS. High-Ca rhodonite up to 35% $CaSiO_3$ mole, and high-Mn bustamite up to 69% $MnSiO_3$ mole were found from the Akatani and Ohnagusa mines, and the Kasuga mine, respectively. The chemical heterogeneity in each grain of high-Ca rhodonite and Mn-bearing clinopyroxenes replacing rhodonite from the Nakatatsu mine is remarkable. Three assemblages divided by relative temperatures among studied minerals are proposed after their compositional ranges and mineral associations.

Introduction

Mn-pyroxenoids and clinopyroxenes occur commonly as minor constituents of skarns from Fe, Zn and Pb ore deposits in Japan. Among Mn-pyroxenoids, Ca-rich species, rhodonite and bustamite, are major. High-Ca rhodonites up to 35% $CaSiO_3$ mole associated with johannsenite have been reported from two skarns in the Akatani and the Ohnagusa mines (Matsubara and Kato, 1986).

On bustamite the maximum $MnSiO_3$ mole content hitherto known is 60% from skarn at the Mitsuka deposit in the Kasuga mine (Ohashi and Finger, 1978). Recently we recognized bustamite containing 69% $MnSiO_3$ mole from the same locality.

From Zn- and Pb-bearing skarn at the Nakatenjo area in the Nakatatsu mine is found rhodonite replaced by Mn-bearing clinopyroxene. These Mn-pyroxenoids and clinopyroxenes have usually chemical heterogeneity. Therefore, EDS analyses under the observation of BEI are most suitable in order to determine their chemical compositions. In this paper we discuss the chemical compositions, especially variation range and heterogeneity, of rhodonite, bustamite and Mn-bearing clinopyroxenes, and their assemblages in skarns from the Akatani mine, Niigata Prefecture, the Nakatatsu mine, Fukui Prefecture, the Kasuga mine, Gifu Prefecture, and the Ohnagusa mine, Okayama Prefecture, Japan.

Occurrences

1 The Akatani mine

The Akatani mine is located about 37 km east of Niigata City. The ore deposit

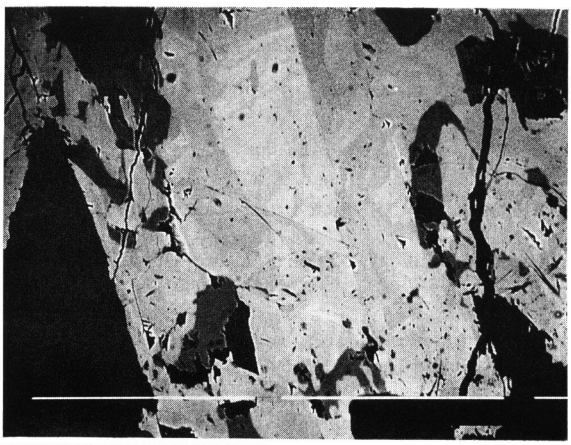

Fig. 1

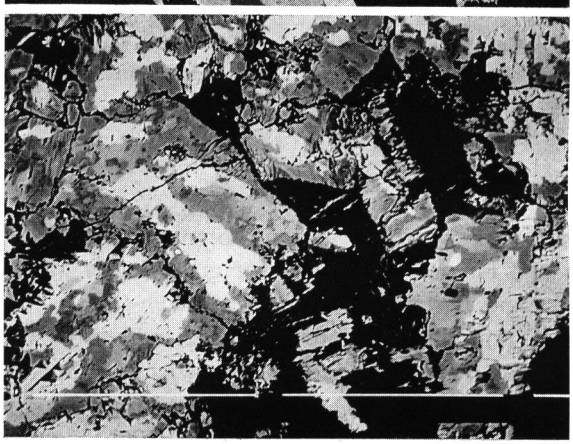

Fig. 2

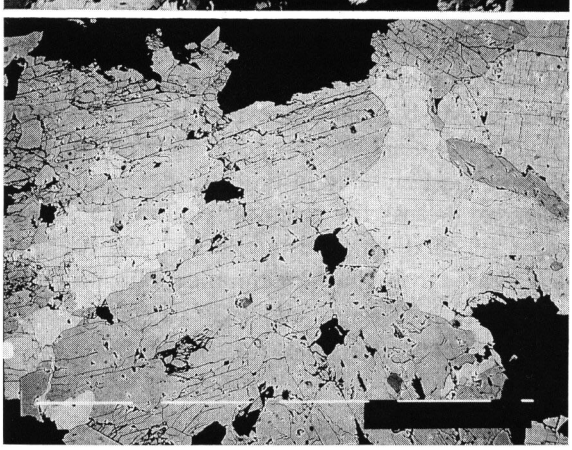

Fig. 3

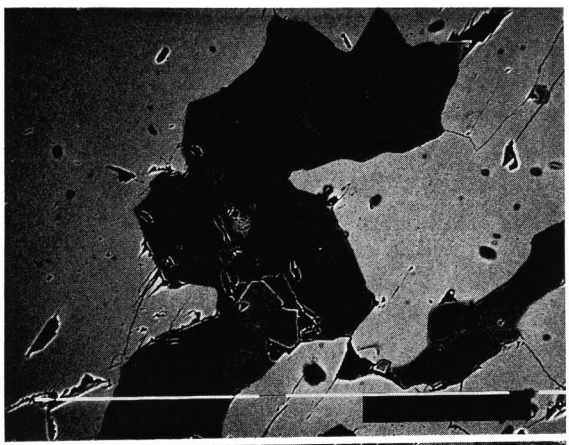

Fig. 4

Fig. 5

Fig. 1. BEI phtograph of rhodonite (white ~ gray), johannsenite (dark gray) and quartz (black) from the Akatani mine. Bar indicates 100 μm.

Fig. 2. BEI photograph of rhodonite (white) replaced by Mn-bearing clinopyroxene (gray) with quartz matrix (black) from the Nakatenjo deposit in the Nakatatsu mine. Bar indicates 100 μm.

Fig. 3. BEI photograph of rhodonite (white), bustamite (gray) and quartz (black) from the Kasuga mine. Bar indicates 100 μm.

Fig. 4. BEI photograph of bustamite (gray) and Mn-bearing clinopyroxene (black) associated with grossular crystals (dark gray) from the Kasuga mine. Bar indicates 100 μm.

Fig. 5. BEI photograph of rhodonite (white ~ gray) from the Ohnagusa mine. Bar indicates 100 μm.

is hydrothermal metasomatic type and is developed in boundary of Neogene rhyolite and Palaeozoic limestone. The detailed geology and deposit have been described by Imai (1960). Hematite had been mined as major ore mineral till about ten years ago, but now the mine produces only calcite powder from recrystallized limestone. Mn-bearing silicates including johannsenite, bustamite and rhodonite occur in coarse

recrystallized limestone as small blocks of skarns. Johannsenite is found as radial aggregates of prismatic crystals up to 15 cm in length. It is light blue to greenish blue on fresh cleavage surfaces, but light brown to yellowish brown in partially altered specimens. In johannsenite prisms are often included aggregates of small pink rhodonite grains. The BEI photograph indicates that rhodonite has remarkable compositional heterogeneity (Fig. 1). Pale bluish green veinlets composed of Mg-rich johannsenite and Mn-rich diopside occur in recrystallized limestone. Along the margin of veinlets very minute fibers of bustamite are often found. It is grey in color and the length is under 0.1 mm. Besides the above minerals manganese silicates-bearing skarn includes galena, sphalerite, chalcopyrite, pyrite, rhodochrosite and quatz as the minor constituents.

2 Nakatatsu mine

The ore deposits of the Nakatastu mine are located about 40 km ESE of Fukui City. Six main ore deposits are known and all are developed in pyroxene and garnet skarns formed by intrusion of Mesozoic quartz porphyry into limestone and shale involved within the Hida marginal zone. The general geology and whole deposits around the Nakatatsu mining area have been summarized by Shimizu and Iiyama (1982). The principal ore includes galena and sphalerite in association with chalcopyrite, pyrrhotite, arsenopyrite, molybdenite, Ag- and Bi-bearing minerals as minor costituents (Nishikawa and Yamaguchi, 1982). The studied specimens were collected from the dumps of the Nakatenjo and Sennou deposits.

Rhodonite from both deposits occurs as pale pinkish aggregates of minute crystals in pyroxene skarn disseminated by small grains of galena, sphalerite, rhodochrosite and quartz. Clinopyroxene is generally found as greenish grey prismatic crystal up to 10 cm in length. It was formed earlier than rhodonite, but minute clinopyroxene replacing the margin of rhodonite crystals is also found from the Nakatenjo deposit (Fig. 2). From the BEI photograph it is considered that the chemical variation range of clinopyroxene is more extensive than rhodonite. The occurrence of bustamite and Mn-bearing pyroxenoids from the Hitokata and Nakayama deposits of this mine are already described (Shimizu and Iiyama, 1982).

3 Kasuga mine

The Kasuga mine is located about 30 km NNW of Gifu City and has three dolomite deposits. One of them is now operated, but the studied specimens were collected from the dump left around the closed deposit near Kawai. Dolomite and limestone have recrystallized to marbles due to contact metamorphism by Mesozoic granite. In dolomite and limestone marbles many skarn minerals such as wollastonite, diopside, grossular, forsterite, phlogopite, clinohumite, pargasite and clinozoisite are recognized as their main constituents. Besides them spinel, geikielite, rutile, chalcopyrite and pyrrhotite are found. Rhodonite occurs as large reddish pink blocks composed of coarse grains up to 1 cm across in association with calcite. It includes rarely minute

bustamite. Prismatic aggregates of bustamite up to 5 cm in length, accompanying Mn-rich diopside, are also found in hornfels. It is pale pink, and the color becomes whiter toward hornfels. Two BEI photographs of clinopyroxene-bustamite and bustamite-rhodonite assemblages indicate that the chemical variation ranges of three species are limited, respectively (Figs. 3 and 4).

4 Ohnagusa mine

The Ohnagusa mine is located about 55 km NW of Okayama City, and the deposit and johannsenite were described by Momoi (1964). The studied specimen was collected from the dump. It is radial aggregate of long prismatic crystals, accompanying small aggregates of rhodonite, kutnohorite and quartz. Rhodonite is generally euhedral, and the compositional heterogeneity is remarkable after the observation of BEI phtograph (Fig. 5).

X-ray powder study

The studied mineral species are identified by the X-ray powder study. Among

Table 1. X-ray powder data for rhodonites

1		2		1		2	
d	I	d	I	d	I	d	I
7.1	50	7.144	30	2.312	4	2.332	8
6.67	15	6.691	25	2.259	3		
4.76	50	4.787	40	2.220	24	2.220	20
4.12	8			2.208	8		
3.81	15	3.837	10	2.178	53	2.185	40
3.55	85	3.576	50	2.152	6		
3.40	11	3.445	15	2.113	11	2.123	15
3.25	12	3.348	35	2.084	7		
3.13	76	3.140	55	2.061	8	2.077	10
3.08	100	3.101	50	1.949	4		
2.969	100	2.990	100	1.892	11	1.907	10
2.925	63	2.953	45	1.860	13	1.879	15
2.809	10	2.812	10	1.831	7		
2.781	26					1.786	8
2.748	46	2.773	15			1.728	8
2.648	18	2.660	15			1.703	10
2.593	34	2.608	30			1.668	20
2.535	7					1.645	5
2.505	65	2.532	40			1.594	8
2.427	10					1.490	10
2.382	8					1.438	25
2.369	16	2.384	10				

1 Magnesian rhodonite from Balmat, New York, USA. (Peacor *et al.*, 1978).
2 High-Ca rhodonite from the Ohnagusa mine, Japan.

Table 2. X-ray powder data for bustamite from the Akatani mine

d	I	d	I
7.544	15	2.433	25
6.921	12	2.289	20
4.870	18	2.248	55*
3.596	35	2.037	15*
3.448	45	1.942	20
3.236	50	1.860	8
3.027	100*	1.720	35
2.647	15	1.572	30
2.550	30*	1.542	20
2.491	25	1.513	20

* enhanced due to admixed Mn-bearing clinopyroxene

Table 3. X-ray powder data for bustamites from the Kasuga mine

1		2		1		2	
d	I	d	I	d	I	d	I
7.493	20	7.468	15	2.143	12	2.116	10
6.910	10	6.889	15	2.115	15	2.091	10
4.870	8	4.854	20	2.040	10	2.022	8
4.445	4	4.423	2	1.976	2		
3.745	50	3.720	70	1.941	12	1.932	12
3.633	5	3.598	4	1.908	4	4.899	2
3.442	60	3.424	100	1.873	8	1.857	10
3.368	5			1.769	8	1.756	8
3.243	100	3.213	100	1.723	35	1.712	50
3.175	8	3.162	8	1.683	15	1.668	15
3.031	55	3.015	60	1.621	5	1.608	8
2.912	20	2.891	20	1.575	5	1.569	4
2.657	30	2.632	35	1.567	8	1.557	5
2.587	5	2.569	5	1.518	5	1.504	5
2.545	10	2.521	8	1.499	15	1.486	15
2.495	35	2.477	50	1.483	12	1.467	10
2.428	15	2.417	15	1.454	10	1.446	4
2.291	15	2.283	15	1.441	12	1.427	8
2.252	60	2.233	85	1.422	15	1.407	15

1 Mn-poor part (38% $MnSiO_3$ mole)
2 Mn-rich part (69% $MnSiO_3$ mole)

them the data for rhodonite (Ohnagusa mine), bustamite (Akatani mine), and Mn-rich and -poor bustamites (Kasuga mine) are given in Tables 1~3. According to the compositional heterogeneity the diffraction peaks of Ohnagusa rhodonite are broad, and shift to lower angles reflecting the high-Ca nature. The diffraction pattern of long prisms of Akatani johannsenite is close to that of ordinary johannsenite near end member. But the diffraction peaks of johannsenite associated with bustamite are

very broad due to the wide chemical variation. Between Mn-rich (69% $MnSiO_3$ mole) and -poor (38% $MnSiO_3$ mole) bustamites the distinct shift of the diffraction peaks is observed in Kasuga material.

Chemical Compositions

The chemical analyses of the studied materials were made by using the Link

Table 4. Representative chemical analyses of rhodonite

Weight percentages:

	Akatani mine		Nakatatsu mine				Kasuga mine		Ohnagusa mine	
			Sennou dep.		Nakatenjo dep.					
SiO_2	46.09	47.56	46.09	46.70	46.73	47.00	47.03	47.74	45.68	46.89
Al_2O_3	0.66	0.30	0	0	0	0	0	0	0.37	0
FeO	1.38	1.30	9.88	7.61	4.28	7.02	0.69	0.56	5.45	1.32
MnO	42.85	37.33	35.81	35.99	42.41	34.47	44.99	42.95	42.30	36.22
MgO	0	0	0.42	0.27	0.41	0.51	0.43	0.46	0.82	0
CaO	9.21	13.90	7.47	9.30	5.97	10.81	7.34	8.98	5.80	14.63
Total	100.19	100.39	99.67	99.87	99.80	99.81	100.48	100.69	100.42	99.06
O=3										
Si	0.98	1.00	0.99	1.00	1.00	1.00	1.00	1.00	0.98	1.00
Al	0.02	0.01	—	—	—	—	—	—	0.01	—
Fe	0.02	0.02	0.18	0.14	0.08	0.12	0.01	0.01	0.10	0.02
Mn	0.78	0.66	0.65	0.65	0.77	0.62	0.81	0.76	0.77	0.65
Mg	—	—	0.01	0.01	0.01	0.02	0.01	0.01	0.03	—
Ca	0.21	0.31	0.17	0.21	0.14	0.25	0.17	0.20	0.13	0.33

Table 5. Representative chemical analyses of bustamite

Weight percentages:

	Akatani mine		Kasuga mine			
			Mn-poor		Mn-rich	
SiO_2	47.66	47.71	48.20	48.46	47.40	47.05
Al_2O_3	0	0	0	0	0	0
FeO	0.51	0.65	4.83	4.59	0.14	0.68
MnO	31.61	31.24	22.27	21.97	38.37	38.56
MgO	0.58	0	1.09	0.88	0.50	0.60
CaO	19.01	19.71	23.30	24.02	12.96	13.23
Total	99.37	99.31	99.69	99.92	99.37	100.12
O=3						
Si	0.99	0.99	0.99	0.99	1.00	0.99
Al	—	—	—	—	—	—
Fe	0.01	0.01	0.08	0.08	0	0.01
Mn	0.57	0.56	0.39	0.38	0.69	0.69
Mg	0.02	—	0.03	0.03	0.02	0.02
Ca	0.42	0.44	0.51	0.53	0.29	0.30

Table 6. Representative chemical analyses of johannsenite

Weight percentages:

	Akatani mine		Ohnagusa mine	
SiO_2	48.10	48.59	47.66	47.96
Al_2O_3	0.46	0	0	0
FeO	1.87	2.23	2.96	3.77
MnO	27.52	26.42	26.38	25.51
MgO	0.47	0.65	0.45	0.45
CaO	21.93	22.35	21.80	21.98
Total	100.35	100.24	99.25	99.67
O=6				
Si	1.98	1.99	1.98	1.99
Al	0.02	—	—	—
Fe	0.06	0.08	0.10	0.13
Mn	0.96	0.92	0.93	0.89
Mg	0.03	0.04	0.03	0.03
Ca	0.97	0.98	0.97	0.98

Table 7. Representative chemical analyses of Mn-rich clinopyroxene

Weight percentages:

	Akatani mine		Nakatatsu mine				Kasuga mine	
			Sennou dep.		Nakatenjo dep.			
SiO_2	49.56	51.37	48.71	51.06	49.27	49.23	50.35	50.40
Al_2O_3	0	0	0	0	0	0	0.41	0.36
FeO	3.23	1.20	13.54	7.47	13.12	17.17	9.23	10.97
MnO	17.88	14.95	13.60	10.66	13.61	10.34	9.72	9.62
MgO	5.55	8.98	1.93	8.19	1.75	1.53	7.19	6.41
CaO	23.21	22.79	22.17	22.43	22.55	22.07	22.89	22.44
Total	99.43	99.29	99.95	99.81	100.30	100.34	99.79	100.20
O=6								
Si	1.98	2.00	1.99	1.99	2.00	2.00	1.98	1.98
Al	—	—	—	—	—	—	0.02	0.02
Fe	0.11	0.04	0.46	0.24	0.45	0.58	0.30	0.36
Mn	0.61	0.50	0.47	0.35	0.47	0.36	0.32	0.32
Mg	0.33	0.52	0.12	0.48	0.11	0.09	0.42	0.38
Ca	0.99	0.95	0.97	0.94	0.98	0.96	0.96	0.95

Systems EDS. In Tables 4 to 7 are given the representative chemical analyses of rhodonite, bustamite, johannsenite and Mn-rich clinopyroxenes, respectively.

The Akatani and Ohnagusa rhodonites associated with near end member johannsenite have two separate ranges of chemical composition, that is, they are located about 20% and 30% $CaSiO_3$ mole, respectively. In the Nakatatsu mine the chemical composition of rhodonite varies from about 15% to 25% $CaSiO_3$ mole and about 8% to 15% (Fe, Mg) SiO_3 mole. Three compositional ranges of the Kasuga bustamite

exist in the present analyses and that of Ohashi and Finger (1978). Bustamite containing 38% $MnSiO_3$ mole was taken from the same specimen studied by Ohashi and Finger (1978). We separated the material accompanying clinopyroxene in close contact with hornfels, but they used the material at the part far from hornfels. The Akatani bustamite is characterized by very low FeO and no MgO contents. Johannsenites from the Akatani and the Ohnagusa mines have nearly same chemical compositions, and their variation ranges are limited. The Nakatatsu and Kasuga clino-

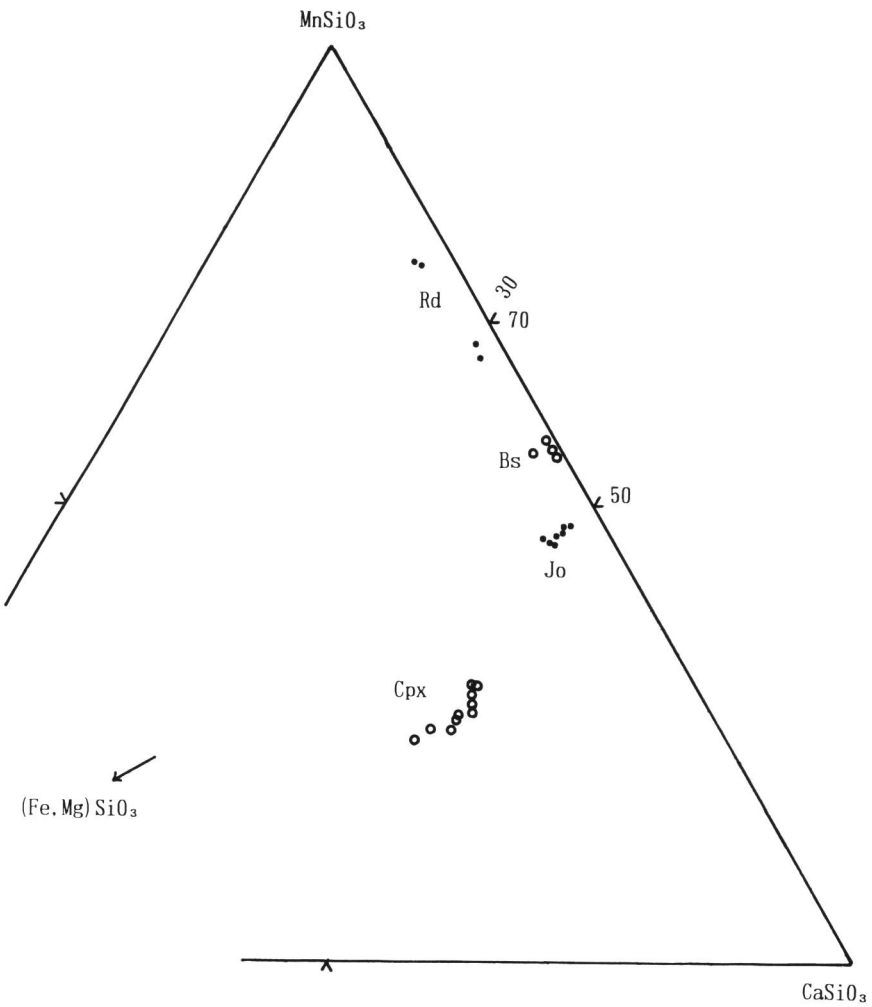

Fig. 6. Rhodonite (Rd), bustamite (Bs), johannsenite (Jo) and Mn-bearing clinopyroxene (Cpx) composition from the Akatani mine plotted in the $MnSiO_3$–$CaSiO_3$–(Fe, Mg)SiO_3 diagram. The assemblages of rhodonite-johannsenite and bustamite-Mn-bearing clinopyroxene are indicated by solid circle and open circle, respectively.

pyroxenes extend their compositional ranges from about 40% to 5% $MgSiO_3$ mole with the mole ratio of $MnSiO_3$: $FeSiO_3 \fallingdotseq 1:1$. But the Akatani clinopyroxene extends its compositional range from about 50% to 30% $MgSiO_3$ mole with about 10% $FeSiO_3$ mole. Rhodonite and clinopyroxene from the Sennou deposit in the Nakatatsu mine include no ZnO, though accompanying zincian rhodochrosite contains up to 19% $ZnCO_3$ mole.

Discussion

The result of chemical analyses of studied minerals from four mines are plotted

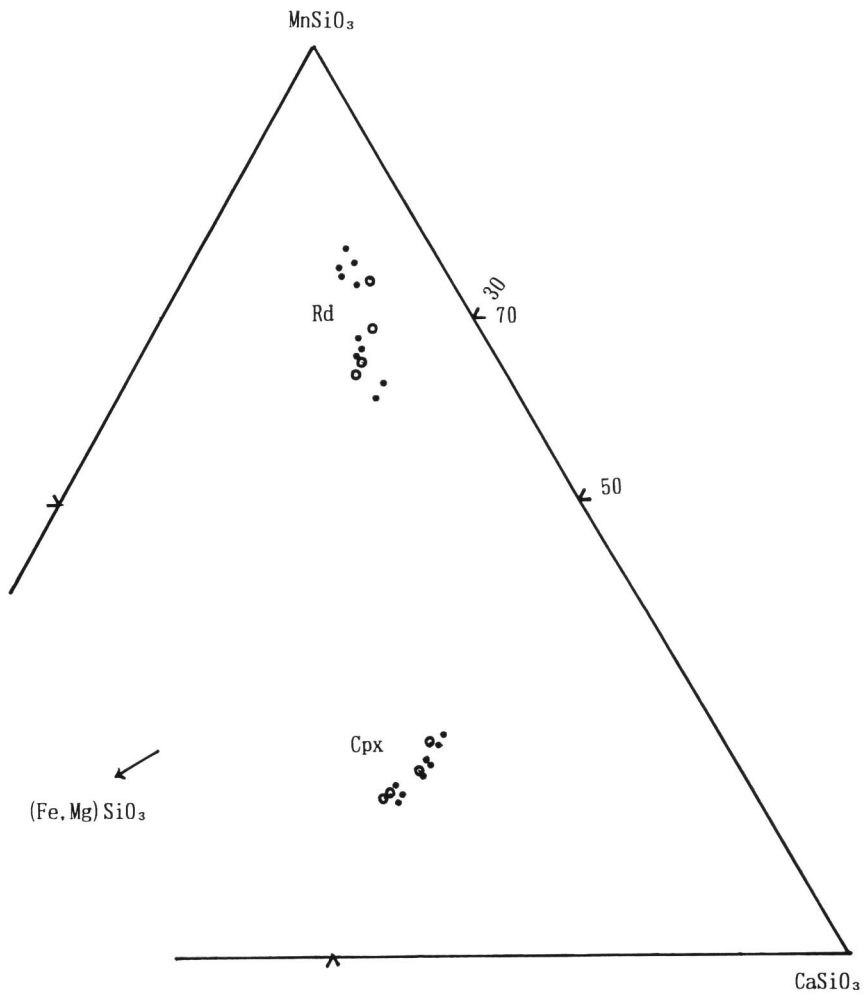

Fig. 7. Rhodonite (Rd) and Mn-bearing clinopyroxene (Cpx) compositions from the Sennou deposit (open) and the Nakatenjo deposit (solid) in the Nakatatsu mine.

in the $MnSiO_3$–$CaSiO_3$–(Fe, Mg)SiO_3 diagrams, respectively (Figs. 6～9). Clinopyroxenes are also plotted in the Jo–Hd–Di diagram (Fig. 10). In the Akatani mine johannsenite is in close association with rhodonite inclusive of two main compositional areas in every grain. One is varying from 30% to 31%, the other from 20% to 21% $CaSiO_3$ mole, both under 3% (Fe, Mg)SiO_3 mole. Mn- poor johannsenite accompanies unusual bustamite whose composition is characterized in very low FeO and no MgO. Because common bustamites from metamorphosed bedded manganese ore deposits in Japan include (Fe, Mg)SiO_3 mole varying from 10% to 20%, where Fe>Mg. The

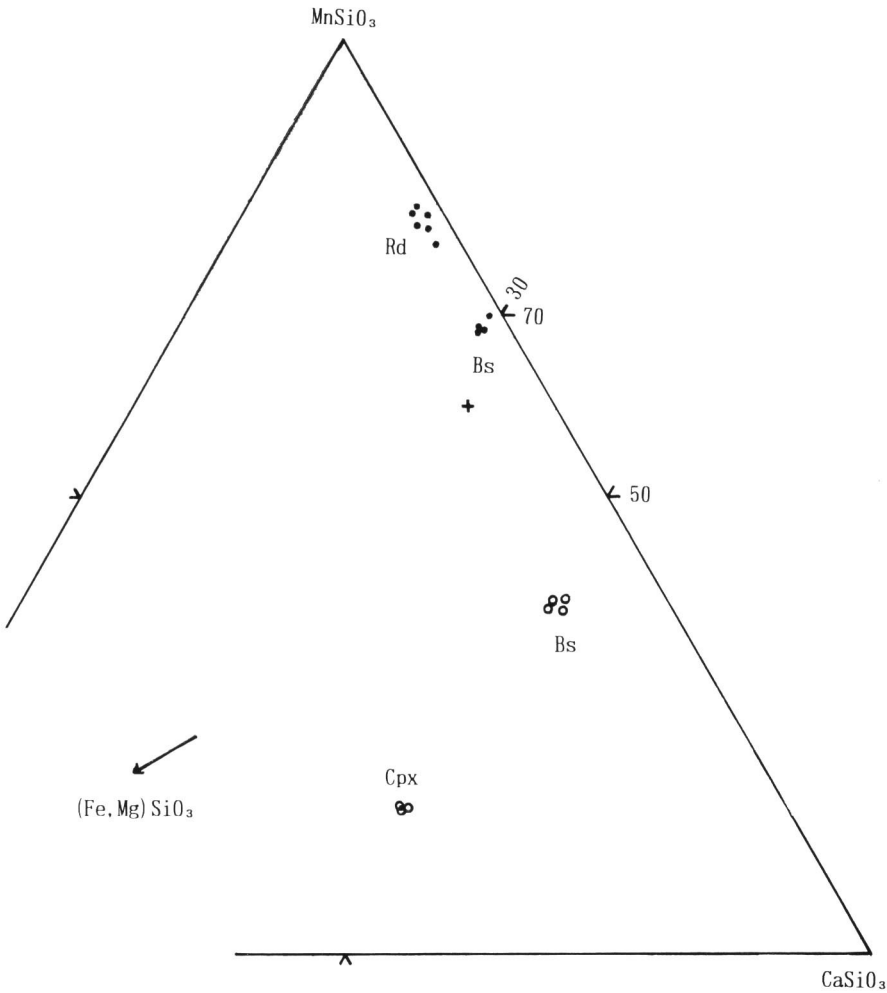

Fig. 8. Rhodonite (Rd), bustamite (Bs) and Mn-bearing clinopyroxene (Cpx) compositions from the Kasuga mine. The assemblages of rhodonite-bustamite and bustamite-Mn-bearing clinopyroxene are indicated by solid and open circle, respectively. Cross indicates bustamite composition in the latter assemblage (Ohashi and Finger, 1978).

Nakatatsu rhodonites from two deposits have wide compositional variation ranges from 15% to 25% $CaSiO_3$ mole and from 8% to 15% (Fe, Mg)SiO_3 mole. But, there is no significant difference among the chemical compositions of both rhodonites. Associated clinopyroxenes from both deposits, also, have similar compositions plotted in two separate ranges along the boundary between johannsenite and hedenbergite areas. Bustamite accompanying rhodonite from the Kasuga mine is specified by high MnO and low (Mg, Fe)O (Mg>Fe) content. The maximum MnO content in the present analyses corresponds to the highest $MnSiO_3$ mole (69%) in hitherto reported bustamite. Bustamite associated with manganoan diopside is plotted around

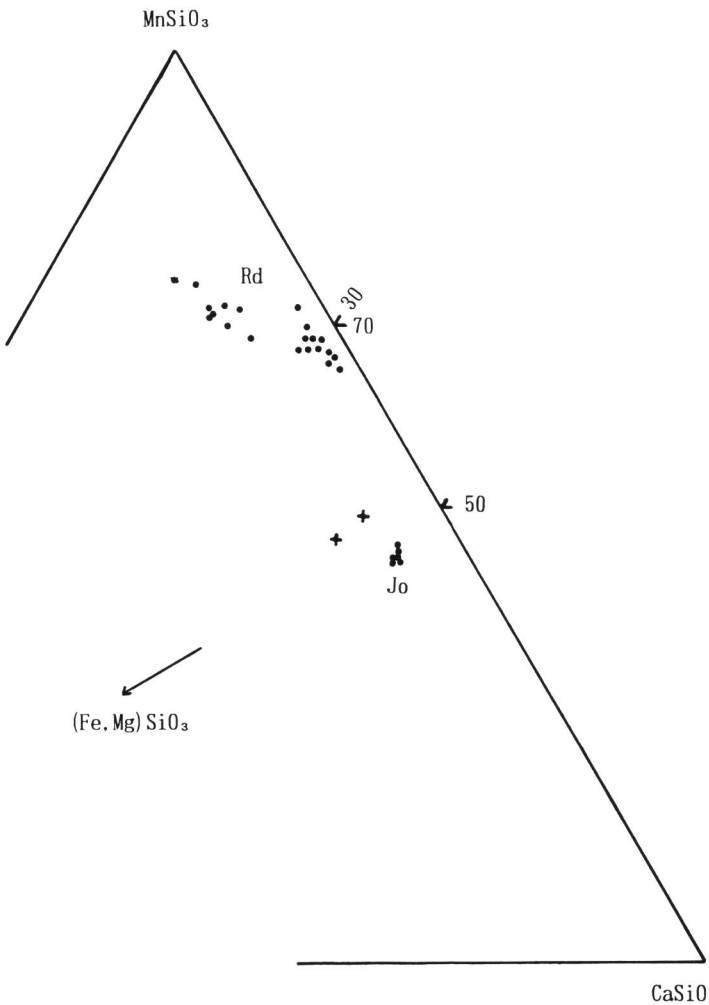

Fig. 9. Rhodonite (Rd) and johannsenite (Jo) compositions from the Ohnagusa mine. Two cross marks indicate johannsenite compositions by Momoi (1964).

38% $MnSiO_3$ mole and 10% (Fe, Mg)SiO_3 mole, but bustamite at the part of about 5 cm apart from manganoan diopside is in the point of 60% $MnSiO_3$ mole and 8% (Fe, Mg)SiO_3 mole (Ohashi and Finger, 1978). This indicates that the homogenization of Ca and Mn is strongly impeded under the condition during formation of ordinary skarn. The Ohnagusa rhodonite has two compositional ranges in one grain, and also the compositional variation in each range is wide. High-Ca type extends from 26% to 33% $CaSiO_3$ mole, wherein the compositional range of the Akatani high-Ca rhodonite is included. But, Ca-poor rhodonite in the Ohnagusa mine has slightly higher (Fe, Mg)SiO_3 mole than that in the Akatani mine. In Fig. 9 two described johannsenite from the Ohnagusa mine by Momoi (1964) are also plotted. Both are considerably Ca-poor in comparison with ordinary johnansenite including the present analyses.

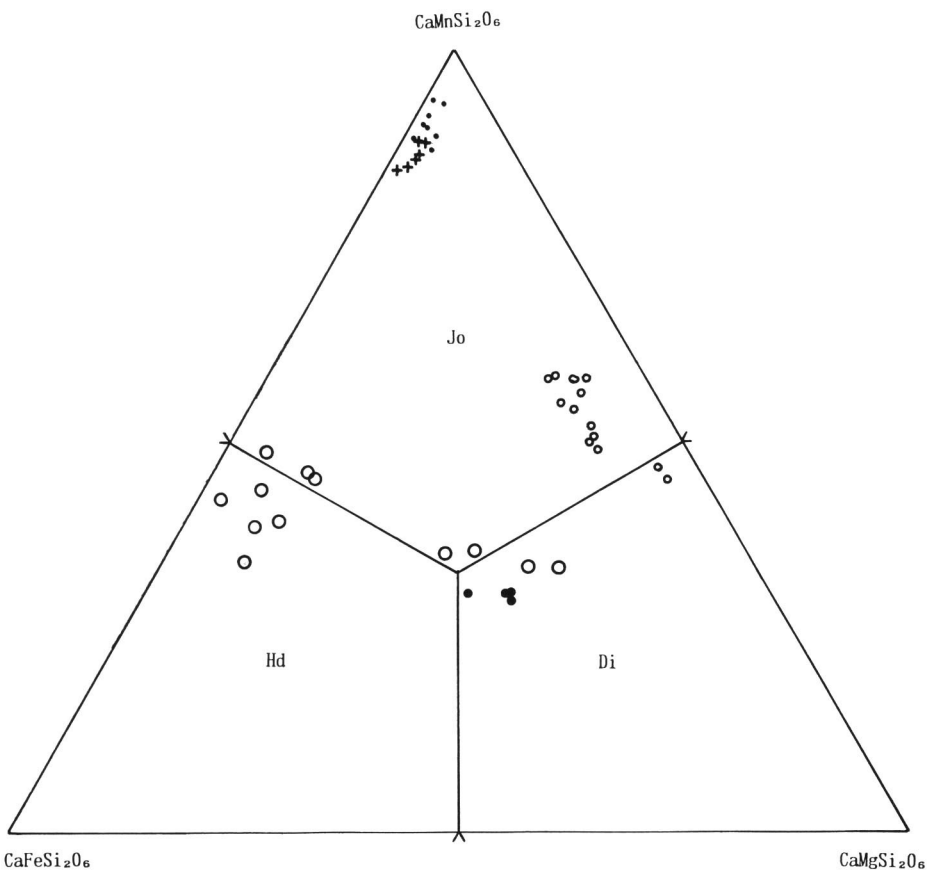

Fig. 10. Mn-bearing clinopyroxene compositions plotted in the $CaMnSi_2O_6$ (Jo)–$CaFeSi_2O_6$ (Hd)–$CaMgSi_2O_6$(Di) diagram. The localities are the Akatani mine (small solid circle and medium open circle), the Nakatatsu mine (large open circle), the Kasuga mine (medium solid circle) and the Ohnagusa mine (cross).

It is very likely that his analysed material included any impurities inviting the decrease of CaO content, probably rhodonite. It seems impossible to prepare a completely pure material after the observation of BEI.

All of the present analyses are plotted in the $MnSiO_3$–$CaSiO_3$–$(Fe, Mg)SiO_3$ diagram (Fig. 11). In this diagram it is notable that both areas of rhodonite and bustamite overlap near the point of 30% $CaSiO_3$ mole and 68% $MnSiO_3$ mole, and also the distribution of clinopyroxene is not consecutive at the range approximately from 10% to 20% $(Fe, Mg)SiO_3$ mole. The $CaSiO_3$ mole range in clinopyroxene

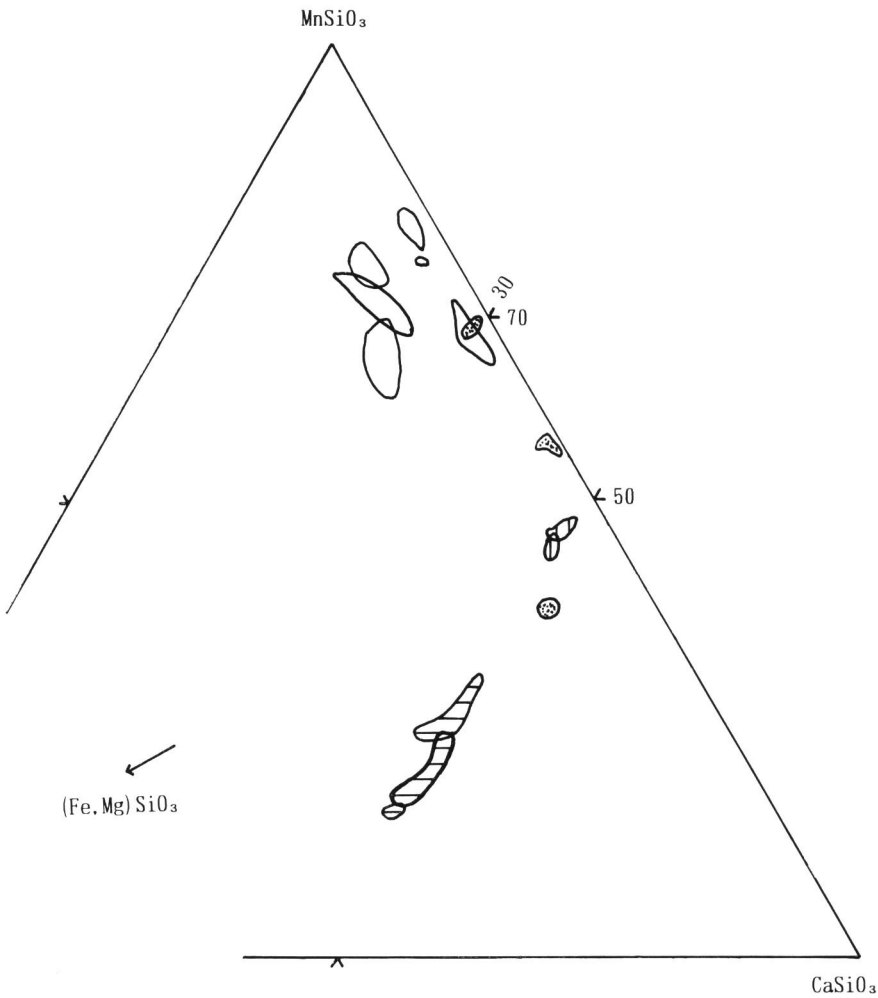

Fig. 11. The compositional ranges of rhodonite (open), bustamite (dotted), johannsenite (vertically lined) and Mn-bearing clinopyroxene (horizontally lined) plotted in the $MnSiO_3$–$CaSiO_3$–$(Fe, Mg)SiO_3$ diagram.

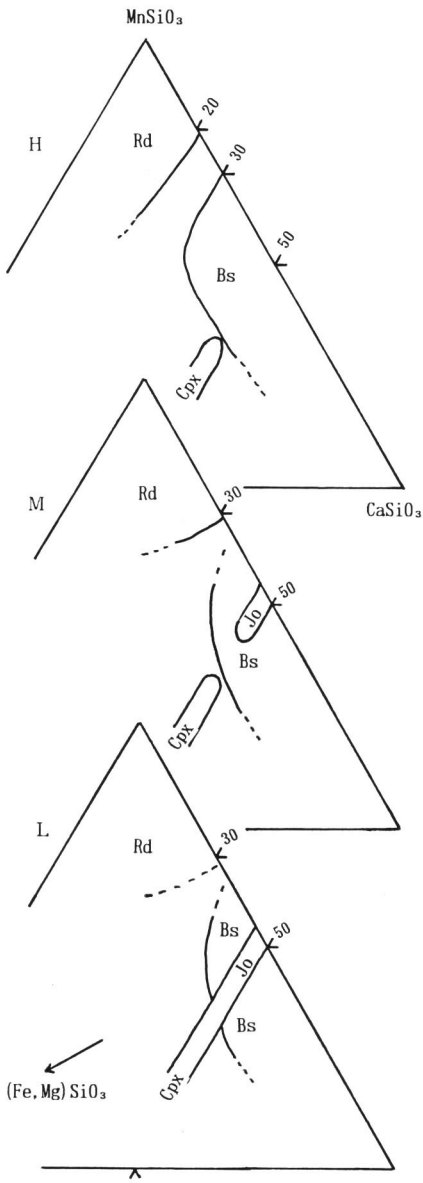

Fig. 12. The idealized assemblage of rhodonite, bustamite, johannsenite and Mn-bearing clinopyroxene divided relative temperatures.

varies from 45% to 50%. The Ohnagusa johannsenite inverts to bustamite after heating (Momoi, 1964; Morimoto *et al.*, 1966). Also, johannsenite is stable under 450°C in experimental studies (Abrecht, 1980; Kakuda *et al.*, 1991). These evidences

lead to the consideration that high-Ca rhodonite and johannsenite near end member are stable at lower temperature, and the increasing temperature invites the extension of stability range of bustamite. The reconstructed assemblages of discussed minerals are given in Fig. 12. Low temperature assemblage probably corresponds to that of Mn-pyroxenoids and Mn-bearing clinopyroxenes in hydrothermal vein type deposits. The formation temperature of these deposits is under 300°C at least. That is, the low temperature assemblage in Fig. 12 indicates the vacant area in experimental studies above 400°C.

Acknowledgement

The part of this study was financially supported by a Grant-in-Aid for Scientific Research (C) from the Ministry of Education, Science and Culture of Japan (Project No. 02640645).

References

ABRECHT, J., 1980. Stability relations on the system $CaSiO_3$–$CaMnSi_2O_6$–$CaFeSi_2O_6$. Contrib. Mineral. Petrol., **74**: 253–260.

IMAI, N., 1960. Relation between ores and altered rocks in so-called contact deposits of the Inner Zone of north eastern Japan. Mining Geol., **10**: 210–226 (In Japanese).

KAKUDA, Y., E. UCHIDA and N. IMAI, 1991. Experimental study on phase equilibria in the system $CaSiO_3$–$MnSiO_3$–(Ca, Mn)Cl_2–H_2O by means of ion exchange. Mining Geol., **41**, 339–349.

MATSUBARA, S. and A. KATO, 1986. High-calcian rhodonite. Abst. Autumn Meeting of Mining Soc. Japan. Assoc. Petrol. Miner. Econ. Geol. Japan, and Miner. Soc. Japan, Mito. 68 (In Japanese).

MOMOI, H., 1964. Johannsenite from Teragochi, Okayama Prefecture, Japan. Mem. Fac. Sci. Kyushu Univ., Ser. D, **15**: 65–72.

MORIMOTO, N., K. KOTO and T. SHINOHARA, 1966. Oriented transformation of johannsenite to bustamite. Mineral. Journ., **5**: 44–64.

NISHIKAWA, Y. and M. YAMAGUCHI, 1982. Zonal distribution of silver-bearing minerals in the skarn type deposits, Nakatatsu mine and its application to ore exploration. Mining Geol., **32**: 203–214 (In Japanese).

OHASHI, Y. and L. W. FINGER, 1978. The role of octahedral cations in pyroxenoid crystal chemistry. I. Bustamite, wollastonite, and the pectolite-schizolite-serandite series. Amer. Mineral., **63**: 274–288.

PEACOR, D. R., E. J. ESSENE, P. E. BROWN and G. A. WINTER, 1978. The crystal chemistry and petrogenesis of a magnesian rhodonite. Amer. Mineral., **63**: 1137–1142.

SHIMIZU, M. and T. IIYAMA, 1982. Zinc-lead skarn deposits of the Nakatatsu mine, Central Japan. Econ. Geol., **77**: 1000–1012.